

Structural characterization of $\text{SiO}_2\text{-Na}_2\text{O-CaO-B}_2\text{O}_3\text{-MoO}_3$ glasses

D. Caurant, O. Majérus, E. Fadel, M. Lenoir
*CNRS, ENSCP, Laboratoire de Chimie de la Matière Condensée de Paris
(UMR-CNRS 7574), 75231 Paris, France*

C. Gervais
*CNRS, Université Pierre et Marie Curie, Laboratoire de Chimie de la Matière Condensée de
Paris (UMR-CNRS 7574), 75252 Paris, France*

T. Charpentier
*CEA Saclay, Laboratoire de Structure et Dynamique par Résonance Magnétique,
DSM/DRECAM/SCM-CEA/CNRS URA 331, 91191 Gif sur Yvette, France*

D. Neuville
*Laboratoire de Physique des Minéraux et Magmas CNRS-IPGP, 4 Place Jussieu,
75252, France*

Nuclear spent fuel reprocessing generates high level radioactive waste with high Mo concentration that are currently immobilized in borosilicate glass matrices containing both alkali and alkaline-earth elements [1]. Because of its high field strength, Mo^{6+} ion has a limited solubility in silicate and borosilicate glasses and crystallization of alkali or alkaline-earth molybdates can be observed during melt cooling or heat treatment of glasses [2-4]. Glass composition changes can significantly modify the nature and the relative proportions of molybdate crystals that may form during natural cooling of the melt. For instance, in a previous work we showed that CaMoO_4 crystallization tendency increased at the expenses of Na_2MoO_4 when B_2O_3 concentration increased in a $\text{SiO}_2\text{-Na}_2\text{O-CaO-MoO}_3$ glass composition [4]. In this study, we present structural results on two series (M_x , B_y) of quenched glass samples belonging to this system using ^{29}Si , ^{11}B , ^{23}Na MAS NMR and Raman spectroscopies. The effect of MoO_3 on the glassy network structure is studied and its structural role is discussed (M_x series). The evolution of the distribution of Na^+ ions within the borosilicate network is followed when B_2O_3 concentration increased (B_y series) and is discussed according to the evolution of the crystallization tendency of the melt. For all glasses, ESR was used to investigate the nature and the concentration of paramagnetic species.

GLASS PREPARATION AND CHARACTERIZATION METHODS

Two series of glasses were prepared for this study all derived from the following composition (mol.%): $58.2\text{SiO}_2 - 13.77\text{Na}_2\text{O} - 9.81\text{CaO} - 18.08\text{B}_2\text{O}_3$ either by increasing MoO_3 concentration from 0 to 5.0 (M_x series with $x = 0, 0.87, 1.54, 2.50, 3.62$ and 5 mol.% MoO_3) or by changing B_2O_3 concentration from 0 to 24 mol.% (B_y series with $y = 0, 6, 12, 18$ and 24 mol.% B_2O_3) keeping constant MoO_3 concentration (2.50 mol.%). For all samples, 0.15 mol.% Nd_2O_3 was introduced in composition both to facilitate ^{29}Si nuclei relaxation during MAS NMR experiments and to perform optical studies not presented in this paper [4]. Glasses were all prepared at 1300°C under air in Pt crucibles using reagent grade SiO_2 , CaCO_3 , Na_2CO_3 , H_3BO_3 , MoO_3 and Nd_2O_3 powders. Depending on glass composition, samples were quenched either as cylinders or disks [4]. Several reference glass samples (borate and silicate glasses) were also prepared for comparison with M_x and B_y glasses (NMR and Raman spectra). The amorphous character of samples was checked using both X-ray diffraction

(XRD) and Raman spectroscopy. Unpolarized Raman spectra of monolithic samples were collected with T64000 Jobin-Yvon confocal Raman spectrometer operating at approximately 1.5 W at room temperature with the 488 nm line of an argon ion laser for excitation. ^{29}Si MAS NMR spectra were recorded on a Bruker Avance 300 spectrometer operating at 59.63 MHz. ^{11}B MAS NMR spectra were recorded on a Bruker Avance 400 operating at 128.28 MHz. ^{23}Na MAS NMR spectra were recorded on a Bruker Avance II 500WB spectrometer operating at 132.03 MHz. Chemical shifts were determined relative to tetramethylsilane for ^{29}Si , liquid BF_3OEt_2 for ^{11}B and 1.0M aqueous NaCl solution for ^{23}Na . ESR spectra were recorded on a Bruker ELEXYS E500 spectrometer operating at X band (9.5 GHz) in the range of temperature 20-300 K. For all glasses of M_x and B_y series, ESR showed the existence of a signal due to Mo near $g\sim 1.91$ and that can be detected at least from 20K to room temperature. These ESR characteristics indicated that this signal is due to paramagnetic Mo^{5+} ($4d^1$) ions located in low symmetry sites. Indeed, the spin-lattice relaxation time of d^1 ions is known to increase (and thus the possibility to detect the ESR signal at high temperature also) with the distortion of the sites. This result is in agreement with the paper of Farges et al. [5] which proposed that the ESR signal of Mo in glasses was associated with low symmetry molybdenyl entities. No signal associated with Mo^{3+} ($4d^3$) ions near $g\sim 5.19$ was detected on ESR spectra [5]. For instance, at 20K only a low intensity contribution due to Nd^{3+} and Fe^{3+} (impurity) ions was detected in the low field region of the spectra. The proportion of Mo^{5+} ions (over all molybdenum) ranges between 0.4 and 0.8 % for all the glasses studied in this work as estimated using a DPPH sample as concentration standard. Consequently, the majority of molybdenum (> 99%) occurs as Mo^{6+} ions in glasses of M_x and B_y series prepared under air (oxidizing conditions). According to Mo EXAFS and XANES results in silicate glasses and to bond valence-bond length considerations published in literature, Mo^{6+} ions are present as tetrahedral molybdate entities MoO_4^{2-} in modifiers rich regions of the glass structure (depolymerized regions) and are not linked directly to the silicate network [1,5,6].

STRUCTURAL EVOLUTION OF GLASSES WITH INCREASING MoO_3 CONCENTRATION

Raman spectra confirm the XRD results presented in [4] showing that the solubility limit of molybdenum in M_x glasses was reached between 1.54 and 2.5 MoO_3 mol.%. Indeed, Fig. 1 clearly reveals the occurrence of the contribution of CaMoO_4 (powellite) Raman vibration modes for $x > 1.54$ mol.%. For comparison, the Raman spectrum of a powellite ceramic sample is given with the attribution of the bands according to [7]. All the CaMoO_4 bands with frequency $\geq 321 \text{ cm}^{-1}$ correspond to internal vibrational modes of MoO_4^{2-} tetrahedra and the strongest band at 879 cm^{-1} can be associated with the symmetric stretching vibration of Mo-O bonds. By analogy, we propose that the wide and intense band observed in the $898\text{-}913 \text{ cm}^{-1}$ range on the Raman spectra of all glasses of M_x series (and also of the B_y series) is also due to the symmetric stretching vibration of Mo-O bonds of molybdate tetrahedra within the glass structure. Fig. 2 indicates that this band moves towards lower frequencies when x increases ($x \geq 2.5$) which shows that the environment and/or the symmetry of MoO_4^{2-} tetrahedra in the glass is modified at least when the crystallization of powellite is detected. Comparison of M_x spectra with the spectrum of a glass without Ca^{2+} ions and belonging to the $\text{SiO}_2\text{-Na}_2\text{O-MoO}_3$ system ($B_0(\text{Na})$ glass in Fig. 2) seems to indicate that the amount of Na^+ ions acting as charge compensators near MoO_4^{2-} tetrahedra increases with x at the expenses of Ca^{2+} ions. This evolution can be explained by the increase of the Na/Ca ratio in the modifiers-rich regions of the glass structure when powellite is formed. Thus, Raman spectroscopy of glasses containing Mo seems to be more sensitive than EXAFS to detect local composition variations around MoO_4^{2-} tetrahedra (and thus symmetry modifications) in the glass structure. Indeed, the Mo

EXAFS results published in literature gave very similar Mo-O distance for different silicate glass compositions (1.76-1.78 Å) [1,5,6].

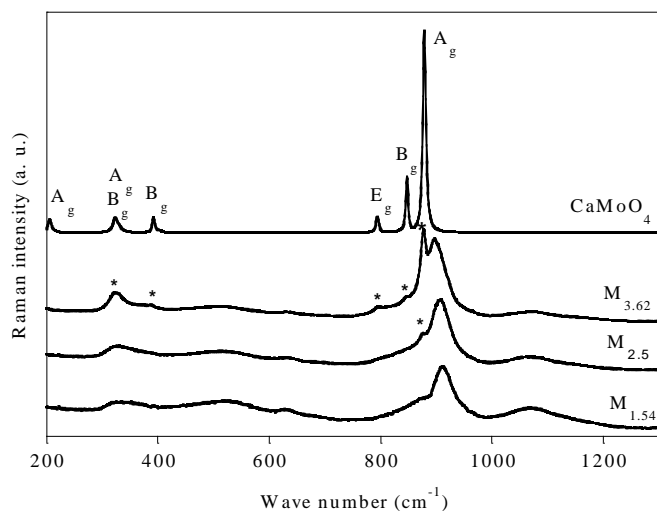


Fig. 1. Normalized Raman spectra of $M_{1.54}$, $M_{2.5}$ and $M_{3.62}$ glasses. The Raman spectrum of a CaMoO_4 (powellite) ceramic is given for comparison. Spectra were not corrected with the Long formula. *: vibration bands due to CaMoO_4 crystals in M_x samples.

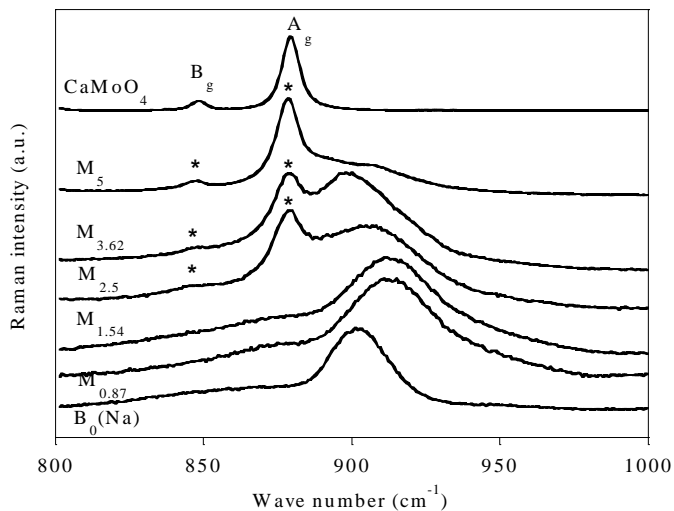


Fig. 2. Normalized Raman spectra of $M_{0.87}$, $M_{1.54}$, $M_{2.5}$, $M_{3.62}$ and M_5 glasses. The spectra of a CaMoO_4 (powellite) ceramic and of sodium silicate glass with Mo (69.34 SiO_2 - 28.09 Na_2O - 2.43 MoO_3 - 0.15 Nd_2O_3 in mol.%) are given for comparison. *: vibration bands due to CaMoO_4 crystals in M_x samples.

^{29}Si MAS NMR spectra were simulated with three bands centered at -80.0, -92.2 and -103.6 ppm respectively associated with Q_2 , Q_3 and Q_4 units (Q_n units with $n = 0$ to 4 correspond to SiO_4 tetrahedra with n bridging oxygen atoms). These chemical shift values were kept constant for the simulation of the spectra of all samples of M_x and B_y series. An example of curve-fitting is shown in Fig. 3a and the evolution of the relative proportions $[Q_n]$ of Q_n units is shown in Fig. 3b. This evolution reveals that $[Q_2]$ and $[Q_3]$ decrease whereas $[Q_4]$ increases when molybdenum concentration increases in samples of the M_x series: when MoO_3 increases from 0 to 5 mol.%, the proportion of Q_4 units increases of more than 20 % (Table 1).

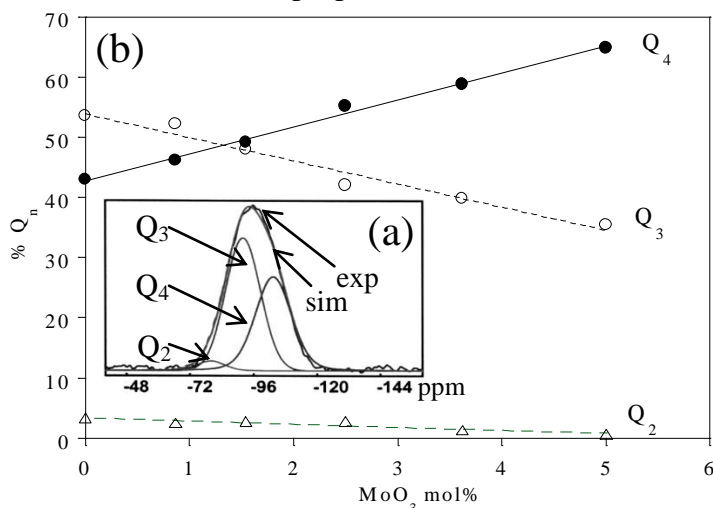


Fig. 3. (a) Example of ^{29}Si MAS NMR spectra recorded for the M_0 sample. The corresponding simulation using three Gaussian line shape contributions associated with Q_2 , Q_3 and Q_4 units is shown (exp: experimental spectrum, sim: simulated spectrum). The same chemical shift values were used for the spectra simulation of all the samples of M_x and B_y series. (b) Evolution of the relative proportions of Q_4 , Q_3 and Q_2 units in M_x samples with the increase of MoO_3 concentration. Linear fits of Q_n evolution are shown.

For the M_x series, ^{11}B MAS NMR spectra simulation only shows a slight and non-monotonous decrease of the relative proportion of BO_4^- units when molybdenum concentration increases: the variation of the proportion of BO_4^- units was only about 2-4 % (Table 1). Consequently, MoO_3 acts as a reticulating agent for the silicate network in M_x glasses and MoO_3 mainly acts on the amount of Q_3 units (Table 1). This result can be explained as follows. As molybdenum is introduced as MoO_3 (corresponding to one Mo^{6+} ion

	M_0	$M_{0.87}$	$M_{1.54}$	$M_{2.50}$	$M_{3.62}$	M_5
% Q_4	43	46.2	49.2	55.2	58.8	64.8
% Q_3	53.6	52.2	48.0	42.0	39.8	34.5
% Q_2	3.4	2.6	2.8	2.8	1.4	0.7
n_{Q_3}	31.19	30.38	27.93	24.44	23.16	20.08
n_{Mo}	0	0.87	1.56	2.56	3.75	5.26
Δn_{Q_3}	-	0.81	3.26	6.75	8.03	11.11
$2n_{Mo}$	0	1.74	3.12	5.12	7.5	10.52
% BO_3	46.0	43.8	46.4	47.8	49.7	47.8
% BO_4	54.0	56.2	53.6	52.3	50.3	52.3
$[BO_4]/[BO_3]$	1.17	1.28	1.15	1.09	1.01	1.09

Table 1. Relative proportions of Q_n units ($n = 2, 3, 4$) and (BO_3, BO_4^-) units in M_x samples determined after simulation and integration of ^{29}Si and ^{11}B MAS-MNR spectra respectively. For a constant number of moles of SiO_2 (58.2 in M_0 composition), the number of moles of Mo^{6+} ions (n_{Mo}) and Q_3 units (n_{Q_3}) is reported for M_x samples. The number of moles of Q_3 units that disappeared (Δn_{Q_3}) when x increased (in comparison with M_0 glass) is also reported.

and 3 non-bridging atoms of oxygen (NBO)) in glass batch whereas Mo^{6+} ions are known to occur as MoO_4^{2-} units (corresponding to one Mo^{6+} ion and 4 NBO) both in glass structure and powellite crystals, each Mo^{6+} ion needs to catch one NBO more from the borosilicate network. We thus propose the following reaction scheme between MoO_3 and Q_3 units (initially charge compensated by Na^+ or Ca^{2+} ions) in the melt:



For a constant number of moles of SiO_2 (58.2 in M_0 composition), the number of moles of Mo^{6+} ions (n_{Mo}) and Q_3 units (n_{Q_3}) was calculated for all M_x samples and is reported in Table 1. The comparison of Δn_{Q_3} (the number of moles of Q_3 units that have disappeared in M_x sample in comparison with M_0 sample) with $2n_{Mo}$ (see equation (1)) shows that the values of Δn_{Q_3} and $2n_{Mo}$ remain close to each other when the amount of MoO_3 increases in glass composition which seems to confirm the reaction scheme (1) proposed above.

STRUCTURAL EVOLUTION OF GLASSES WITH INCREASING B_2O_3 CONCENTRATION

In [4] we showed that Na_2MoO_4 crystallization tendency during slow cooling of the melt ($1^\circ C/min$) decreased with the increase of B_2O_3 concentration whereas the tendency of $CaMoO_4$ to crystallize increased. Such an evolution can be explained by the preferential charge compensation of BO_4^- units by Na^+ rather than by Ca^{2+} ions in borosilicate glasses [8]. For the B_y series, Fig. 4 shows that the $[BO_4^-]/[SiO_2]$ ratio increases whereas $[Na^+]/[BO_4^-]$ decreases with B_2O_3 concentration. It is interesting to notice that for the B_{24} sample almost all Na^+ ions can act as BO_4^- charge compensator ($[Na^+]/[BO_4^-] \sim 1$). In these conditions, the amount of Na^+ ions able to compensate the MoO_4^{2-} entities strongly decreases when B_2O_3 concentration increases and the $[Ca^{2+}]/[Na^+]$ ratio in the depolymerized regions of glass structure increases which can be explained by the evolution of the crystallization tendency. Fig. 5 shows that the isotropic ^{23}Na chemical shift ($\delta_{iso}(^{23}Na)$) decreases when B_2O_3 concentration increases. Thus, the distribution of Na^+ ions through the glassy network significantly changes when increasing amounts of boron are introduced in B_y glasses. Comparison of $\delta_{iso}(^{23}Na)$ of B_y glasses with

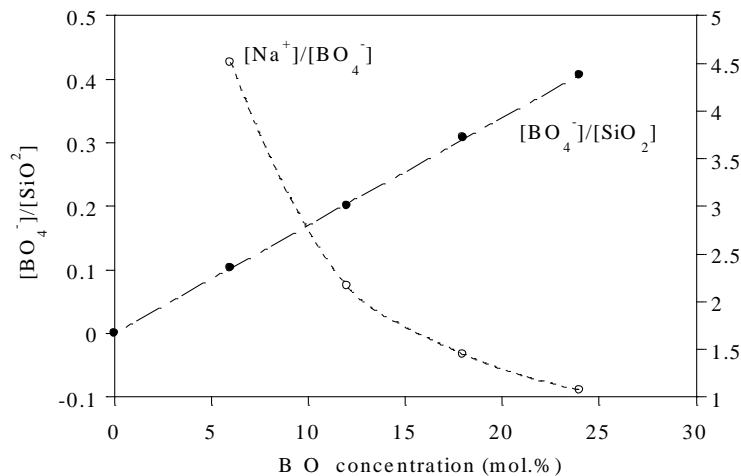


Fig. 4. Evolution of the $[\text{BO}_4^-]/[\text{SiO}_2]$ and $[\text{Na}^+]/[\text{BO}_4^-]$ ratios versus B_2O_3 concentration in B_y samples (mol.%). The Na^+ and SiO_2 concentrations were determined by chemical analysis whereas the BO_4^- concentration was determined by chemical analysis and ^{11}B MAS NMR.

that of sodium silicate (SiNa), sodium calcium silicate (SiNaCa) and borate ($\text{B}_{0.2}\text{Na}$, $\text{B}_{0.7}\text{Na}$) reference glasses clearly reveals that when B_2O_3 concentration increases, Na^+ ions moves from a charge compensator position near NBO to a charge compensator position near BO_4^- units.

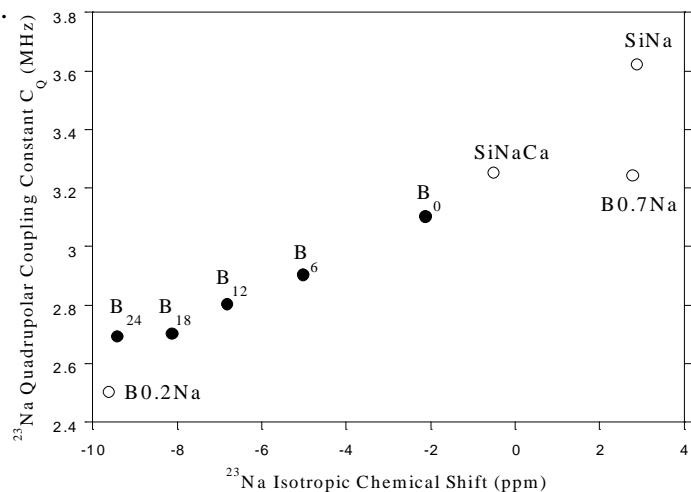


Fig. 5. Evolution of the ^{23}Na isotropic chemical shift (δ_{iso}) and quadrupolar coupling constant (C_Q) in the samples of B_y series. For comparison the values of δ_{iso} and C_Q of reference glasses are also shown: SiNa ($80.93\text{SiO}_2 - 19.07\text{Na}_2\text{O}$), SiNaCa ($71.21\text{SiO}_2 - 16.78\text{Na}_2\text{O} - 12\text{CaO}$), $\text{B}_{0.7}\text{Na}$ ($58.8\text{B}_2\text{O}_3 - 41.2\text{Na}_2\text{O}$), $\text{B}_{0.2}\text{Na}$ ($83.3\text{B}_2\text{O}_3 - 16.7\text{Na}_2\text{O}$). For the three former reference glasses Na^+ ions can compensate NBO whereas in the later one Na^+ ions only compensate bridging oxygen atoms near BO_4^- units.

In accordance with the XRD results on the B_y quenched disk samples, Raman spectra show that the crystallization of CaMoO_4 is detected when B_2O_3 concentration is higher than 12 mol.% (Fig. 6). Contrary to the Raman spectra of the samples of the M_x series, the position of the band associated with Mo-O stretching vibration near 905 cm^{-1} only slightly evolves when B_2O_3 concentration increases which indicates that the environment of MoO_4^{2-} entities is only slightly modified. As the depolymerized regions in which are located MoO_4^{2-} entities become progressively depleted in sodium when B_2O_3 concentration increases, the lack of strong evolution of the M-O vibrational frequency could indicate that MoO_4^{2-} entities are preferentially charge compensated by Ca^{2+} ions.

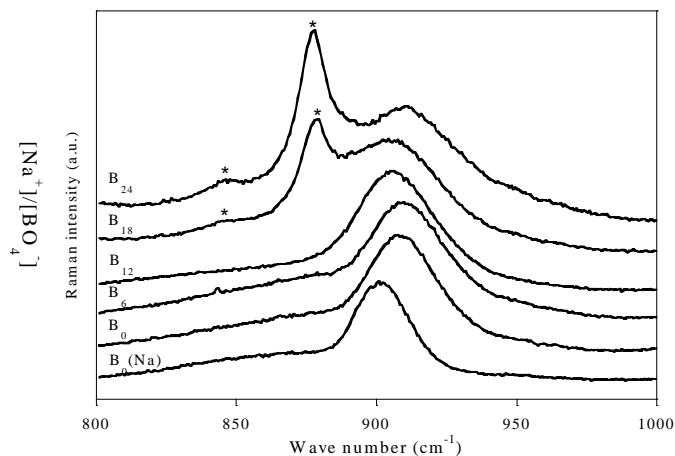


Fig. 6. Evolution of Raman spectra of B_y samples. For comparison the spectrum of the $\text{B}_0(\text{Na})$ reference glass without calcium is also shown. *: vibration bands due to CaMoO_4 crystals in M_x samples.

¹ G. Calas, M. Le Grand, L. Galois, D. Ghaleb, *J. Nucl. Mater.* **322** (2003) 15.

² R. J. Short, R. J. Hand, N. C. Hyatt, *Mat. Res. Soc. Symp. Proc.* **757** (2003) 141.

³ C. Cousi, F. Bart, J. Phallipou, *J. Phys. IV France* **118** (2004) 79.

⁴ D. Caurant, O. Majerus, E. Fadel, M. Lenoir, C. Gervais, O. Pinet, *J. Am. Ceram. Soc.* **90** (2007) 774.

⁵ F. Farges, R. Siewert, G. E. Brown, A. Guesdon, G. Morin, *The Canadian Mineralogist* **44** (2006) 731.

⁶ N. Sawaguchi, T. Yokokawa, K. Kawamura, *Phys. Chem. Glasses* **37** (1996) 13.

⁷ E. Sarantopoulou, C. Raptis, S. Ves, D. Christofilos, G. A. Kourouklis, *J. Phys. Condens. Matter* **14** (2002) 8925.

⁸ A. Quintas, T. Charpentier, O. Majerus, D. Caurant, J-L. Dussossoy, *Appl. Magn. Reson.* **32** (2007) 613-634.